



Published in final edited form as:

*Biomaterials*. 2017 July ; 132: 59–71. doi:10.1016/j.biomaterials.2017.04.004.

## Stem cell delivery in tissue-specific hydrogel enabled meniscal repair in an orthotopic rat model

Xiaoning Yuan<sup>a</sup>, Yiyong Wei<sup>a,b</sup>, Aránzazu Villasante<sup>a</sup>, Johnathan J.D. Ng<sup>a</sup>, Derya E. Arkonac<sup>a</sup>, Pen-hsiu Grace Chao<sup>c</sup>, and Gordana Vunjak-Novakovic<sup>a,#</sup>

<sup>a</sup>Department of Biomedical Engineering, Columbia University, New York, NY, USA

<sup>b</sup>Department of Orthopaedics, Ruijin Hospital, Shanghai Jiaotong University School of Medicine, Shanghai, China

<sup>c</sup>Institute of Biomedical Engineering, School of Medicine and School of Engineering, National Taiwan University, Taipei, Taiwan

### Abstract

Interest in non-invasive injectable therapies has rapidly risen due to their excellent safety profile and ease of use in clinical settings. Injectable hydrogels can be derived from the extracellular matrix (ECM) of specific tissues to provide a biomimetic environment for cell delivery and enable seamless regeneration of tissue defects. We investigated the *in situ* delivery of human mesenchymal stem cells (hMSCs) in decellularized meniscus ECM hydrogel to a meniscal defect in a nude rat model. First, decellularized meniscus ECM hydrogel retained tissue-specific proteoglycans and collagens, and significantly upregulated expression of fibrochondrogenic markers by hMSCs versus collagen hydrogel alone *in vitro*. The meniscus ECM hydrogel in turn supported delivery of hMSCs for integrative repair of a full-thickness defect model in meniscal explants after *in vitro* culture and *in vivo* subcutaneous implantation. When applied to an orthotopic model of meniscal injury in nude rat, hMSCs in meniscus ECM hydrogel were retained out to eight weeks post-injection, contributing to tissue regeneration and protection from joint space narrowing, pathologic mineralization, and osteoarthritis development, as evidenced by macroscopic and microscopic image analysis. Based on these findings, we propose the use of tissue-specific meniscus ECM-derived hydrogel for the delivery of therapeutic hMSCs to treat meniscal injury.

### Keywords

extracellular matrix; injectable therapies; meniscus; mesenchymal stem cells; animal models

---

<sup>#</sup>Please address correspondence to: Gordana Vunjak-Novakovic, PhD, Columbia University, 622 West 168th Street, VC12-234, New York, NY, 10032. gv2131@columbia.edu.

Appendix A. Supplementary data: Supplementary data related to this article can be found at ...

**Publisher's Disclaimer:** This is a PDF file of an unedited manuscript that has been accepted for publication. As a service to our customers we are providing this early version of the manuscript. The manuscript will undergo copyediting, typesetting, and review of the resulting proof before it is published in its final citable form. Please note that during the production process errors may be discovered which could affect the content, and all legal disclaimers that apply to the journal pertain.

## 1. Introduction

Promising new tissue engineering approaches have incorporated natural biomaterials made from the extracellular matrix (ECM) of decellularized tissues, such as heart [1], lung [2], and bone [3]. Decellularization preserves the molecular composition of the native ECM with tissue-specific molecules, including the structural and mechanical features of the original tissue, which guide the behavior of therapeutic cells and facilitate tissue development [4]. The applications of decellularized biomaterials range from whole organ replacements to tissue patches and hydrogels that can be therapeutic or serve as delivery vehicles for drugs, biologics, or cells [5]. Injectable hydrogels have enabled novel treatment options due to the modes of administration that can be tailored to specific tissues and diseases. One important focus is in sports medicine, where injectable orthobiologics such as hyaluronic acid and platelet-rich plasma [6] are broadly utilized for treating osteoarthritis (OA) and injuries to tendons, ligaments, and menisci. The latter are fibrocartilaginous tissues that specialize in load-bearing and stabilization of the knee joint [7,8].

Meniscal injury is of particular interest, as they are implicated in over half of all arthroscopic procedures performed by orthopaedic surgeons [9], the majority of which involves surgical resection (partial meniscectomy), despite knowledge that partial removal of meniscal tissue contributes to the development of OA [10].

Given the importance of the meniscus in the biomechanics of the knee, and the role of meniscus ECM in maintaining the functional properties of meniscal tissue, repair of the meniscus must regenerate the native ECM. In the subpopulation of patients with meniscal damage but otherwise healthy knee joints, meniscal replacement has been studied by implanting tissue allografts [11], synthetic biomaterials [12–14], and decellularized xenografts [15–18]. However, it has long been appreciated that the dense ECM of the meniscus obstructs cellular infiltration and integration. In a canine model, cells were shown to repopulate devitalized meniscal allografts, but the central core of the tissue remained acellular even at six months after transplantation [19]. Cell migration into the decellularized meniscus was limited to ~150  $\mu\text{m}$  over seven days *in vitro*, precluding robust tissue formation [20].

To overcome these limitations, we developed a hydrogel from decellularized bovine meniscus ECM to deliver human mesenchymal stem cells (hMSCs) into full-thickness defects in explant models *ex vivo* and animal models *in vivo*, and promote growth of viable repair tissue. Mesenchymal stem cells (MSCs) were selected for our study as they have been widely studied in musculoskeletal diseases [21–23], with previous clinical reports on their use in meniscal repair and OA treatment [24,25]. To improve repair outcomes, hMSCs need to differentiate and grow new tissue, and to produce trophic factors for tissue remodeling and regeneration. Intra-articular delivery of cells has been previously applied in pre-clinical [26–31] and clinical [25,32–34] studies of various osteochondral conditions. However, without an appropriate carrier, large numbers of cells need to be injected to compensate for the massive cell loss by dispersion from the defect site [29]. We hypothesized that a hydrogel derived from decellularized meniscus ECM (mECM) can protect exogenously delivered cells, localize them to the site of injury, and provide signals for the formation of

new repair tissue. To test this hypothesis, we investigated the development of meniscal tissue by hMSCs in mECM and collagen hydrogels *in vitro*, and the capacity of hMSC-mECM hydrogel constructs to integrate with native meniscus *in vitro* and *in vivo*, and to repair meniscal injury in an orthotopic nude rat model.

## 2. Materials and Methods

### 2.1. Culture of human mesenchymal stem cells

hMSCs were isolated from fresh, unprocessed human bone marrow aspirates (Lonza, Basel, CH), and characterized as previously described [3]. Cells were expanded to passages 4-5 in basal medium consisting of high glucose (hg) DMEM, 10% fetal bovine serum (FBS), 1× antibiotic-antimycotic, and 0.1 ng/mL bFGF (Thermo Fisher Scientific, Waltham, MA).

### 2.2. Decellularization and digestion of bovine meniscus extracellular matrix

Juvenile bovine menisci were dissected within 36 h of slaughter (Green Village Packing Company, Green Village, NJ), minced to 1-2 mm<sup>3</sup> pieces, and lyophilized for 24 h. Tissues were decellularized at 25°C with agitation in 2% SDS and 10 mM Tris (3 cycles, 24 h each), followed by 0.1% peracetic acid (2 h), washed with sterile water and PBS (3 cycles), and lyophilized again (24 h). The resulting meniscus ECM (mECM) was digested at an initial concentration of 40 mg/mL at 25°C with agitation in 0.1% pepsin + 0.01 M HCl (12 h), resulting in a mECM digest solution. Biochemical analysis confirmed the retention of ECM constituents and removal of DNA (Figure S1). The mECM digests, along with type I collagen controls (BD Biosciences, San Jose, CA) and Precision Plus Protein Dual Color Standards (Bio-Rad, Hercules, CA), were analyzed by SDS-PAGE on 4-20% gels (Bio-Rad), stained with Coomassie Brilliant Blue (Bio-Rad), and imaged by a Canon imageCLASS D480 (Melville, NY; Figure S2).

### 2.3. Encapsulation of hMSCs in hydrogel

For hydrogel studies, mECM digests and type I collagen (rat tail; BD Biosciences) were gelled based on a previously established protocol [4]. Briefly, type I collagen hydrogels (3 mg/mL) were formed by mixing collagen solution (30% by volume), 0.1 N NaOH (3%), 10× PBS (3.3%), hgDMEM (63.7%) at physiologic pH and 4°C. Similarly, mECM hydrogels (5.61 mg/mL) were formed by mixing mECM digest (56% by volume), 0.1N NaOH (5.6%), 10× PBS (6.2%), hgDMEM (32%) at 4°C. The concentration of mECM in hydrogel (5.61 mg/mL) was chosen to match the hydroxyproline content of the type I collagen hydrogel (3 mg/mL), as quantified by a modified acid hydrolysis assay [35].

hMSCs were encapsulated in type I collagen or mECM hydrogels at 30×10 cells/mL, then injected in 25 µL aliquots into 4-mm diameter poly(dimethylsiloxane) rings. Gelation occurred over 40 min at 37°C, and subsequent hMSC-laden constructs in either mECM or type I collagen hydrogel were cultured for 28 days in chondrogenic media (CM), containing hgDMEM, 1× antibiotic-antimycotic, 0.1 µM dexamethasone, 50 µg/mL ascorbate 2-phosphate, 40 µg/mL L-proline, 100 µg/mL sodium pyruvate, 1× insulin/transferrin/selenium premix (BD Biosciences), with or without 10 ng/mL TGF-β3 (PeproTech, Rocky

Hill, NJ). Samples were collected at days 0, 14, and 28 for biochemical, histological, and gene expression analyses.

#### 2.4. Mechanical integration testing in an *in vitro* tissue-explant model

Juvenile bovine menisci were dissected as previously described [36]. Explants were harvested from the central tissue region using sterile 4 mm diameter biopsy punches, and cut to 1.5 mm height using a custom microtome device. A 1.5-mm diameter central core was punched out, leaving a tissue ring. Explant rings were devitalized at 4°C with agitation in sterile water (5 cycles, 24 h each, sterile water changes between cycles) [37]. hMSCs were encapsulated in mECM hydrogel as described above, and after 3 days of culture in basal medium, two hMSC-laden mECM gels were press-fitted into the devitalized rings. mECM-explant composites were cultured for 42 days in CM with 10 ng/mL TGF-β3. Samples were collected at timed intervals for mechanical, biochemical and histological analyses.

Integration of full-thickness defects in meniscus explants was tested using a custom device consisting of a 1.33-mm diameter indenter in series with a 50 g load cell, placed above a cup with a 2 mm diameter hole using our previously established protocol [38]. Prior to testing, the height of each sample was measured using a digital caliper. The indenter was displaced at a ramp rate of 0.3% of the sample height per second, until the central core was pushed fully through the outer ring. Integration strength was calculated as the ratio of the peak force to the surface area of contact between the central core and outer ring.

#### 2.5. Phenotype stability in a subcutaneous implantation model in nude mouse

After 6 weeks of *in vitro* culture, devitalized meniscal explants containing mECM-encapsulated hMSCs were implanted subcutaneously into nude mice for 4 weeks *in vivo*, according to an approved protocol at Columbia University. Female NOD/SCID mice at 6 weeks of age (Harlan, Indianapolis, IN) were anesthetized by intraperitoneal injections of ketamine (80-100 mg/kg) and xylazine (5-10 mg/kg), with analgesia by subcutaneous administration of buprenorphine SR (1.2 mg/kg). Constructs were implanted into separate subcutaneous dorsal pockets (1 construct per pocket, 2 pockets per animal). Implants were collected after 4 weeks *in vivo* and evaluated for expression of chondrogenic, hypertrophic, and osteogenic markers.

#### 2.6. Orthotopic model of meniscal injury in nude rat

A previously published protocol of anterior medial hemi-meniscectomy was adapted for use of human cells in nude rats [29]. Briefly, male athymic nude rats (Hsd:RH-*Foxn1*<sup>tmu</sup>; Harlan) at 14 weeks of age were anesthetized by inhaled isoflurane, with analgesia by subcutaneous buprenorphine. Using aseptic technique, the anterior aspect of the right knee was exposed by a straight incision via a medial parapatellar approach, the patella was temporarily subluxed laterally for access, and the anteromedial joint capsule was cut. The anterior horn of the medial meniscus was dislocated anteriorly and cut radially at the level of the medial collateral ligament without damaging the ligament itself, resulting in the excision of meniscal tissue 2 mm × 2 mm in size. The incision was closed in layers (muscle, subcutaneous tissue, skin), and prior to final closure of the subcutaneous tissue and skin layers, the hMSCs ( $7.5 \times 10^5$  in 50 μL of mECM hydrogel) were injected into the intra-

articular space ( $n = 7$ ). This procedure was repeated for the left knee, which received an intra-articular injection of hMSCs ( $7.5 \times 10^5$ ) in 50  $\mu$ L PBS instead of mECM hydrogel. In control animals ( $n = 3$ ), meniscal tissue was excised bilaterally, but received no further interventions after wound closure. At eight weeks post-injury, all animals were euthanized by CO<sub>2</sub> inhalation and cervical dislocation. Bilateral medial menisci were dissected and preserved at 4°C in 4% formaldehyde for histologic analysis. Radial cross-sections of the regenerated meniscal tissue were used for histological staining. For control samples with minimal tissue regeneration, radial cross-sections were obtained from the most anterior portion of the medial menisci. Quantification of the area of anterior medial meniscus resected and regenerated was performed using Fiji (Madison, WI).

## 2.7. Computed tomography imaging and 3D segmentation of implanted animals

At biweekly time points starting at four weeks post-injury, all animals were imaged in a small animal nanoScan SPECT/CT (single-photon emission computer tomography/computed tomography) system (Mediso, Budapest, HU). Under anesthesia by isoflurane, microCT scanning was performed with focus over the hindlimbs at 4, 6, and 8 weeks post-injury. Three-dimensional segmentation of the CT images was performed with Mimics 17 (Materialise, Leuven, BE). Thresholding masks were applied to highlight bone (lower threshold: -980 to -970 HU; upper threshold: -760 to -770 HU). We obtained indirect measures of left and right knee joint space volumes for each animal at each time point, by calculating the difference between a fixed cubic volume (6 mm  $\times$  4 mm  $\times$  3 mm) and the bone volume.

## 2.8. Gene expression in hMSCs

Cell-laden mECM or collagen gels at days 0, 14, 28 were homogenized by pellet pestle. Total RNA was extracted in TRIzol reagent (Thermo Fisher Scientific) and reverse transcribed (High Capacity cDNA Reverse Transcription Kit; Thermo Fisher Scientific). Subsequent cDNA amplification was performed using an Applied Biosystems StepOnePlus Real-Time PCR System, Fast SYBR Green Master Mix (Thermo Fisher Scientific), and custom human primers for *ACAN*, *COL1A2*, *COL2A1*, *COL10A1*, and *GAPDH* to calculate relative expression ( $2^{-C_T}$ ).

## 2.9. Biochemical content of hydrogel-encapsulated cells

The biochemical compositions of the native and decellularized mECM, mECM digests, and hMSCs encapsulated in mECM and collagen hydrogels were quantified for DNA, sulfated glycosaminoglycan (GAG), and total collagen contents. Briefly, samples were lyophilized for 24 h and digested at 60°C for 16 h in a papain solution containing 125  $\mu$ g/mL papain (Sigma-Aldrich, St. Louis, MO), 50 mmol phosphate buffer (pH 6.5), and 2 mmol *N*-acetyl cysteine (Sigma-Aldrich). The DNA content of sample digests was obtained using the PicoGreen dsDNA quantitation kit (Thermo Fisher Scientific), according to manufacturer's protocol. Sulfated GAG content was measured using the 1,9-dimethylmethylene blue dye-binding assay [39]. Total collagen content was quantified by a modified acid hydrolysis assay [35], using *ortho*-hydroxyproline (OHP) as standards for meniscus ECM and hMSC-laden gels, or type I collagen solution for mECM digests.

## 2.10. Histological analysis

For histological processing, hydrogel-encapsulated hMSCs were embedded in 2% low-melting-temperature agarose and fixed at 4°C in 4% formaldehyde. Samples were dehydrated in a graded series of ethanol, embedded in paraffin, and sectioned to 8 µm thick. Sections were stained with hematoxylin and eosin (H&E) for nuclei and cytoplasmic elements, respectively, Alcian blue (pH 1.0) for sulfated GAGs, and Picrosirius red for collagens. Additionally, implanted samples and rat menisci were stained with von Kossa for mineralization and nuclear fast red for nuclei.

For immunohistochemistry, the following primary antibodies were used for hMSCs in hydrogels and rat menisci: mouse anti-type I collagen (1:200; Abcam, Cambridge, UK); rabbit anti-type II collagen (1:50; Abcam); mouse anti-type X collagen (1:2000; Abcam); and mouse anti-human nuclei (1:50; Millipore). Briefly, all samples were processed using the VECTASTAIN Elite ABC Kit (Universal; Vector Laboratories, Burlingame, CA) and counterstained with hematoxylin QS, with the exception of staining against human nuclei. Antigen retrieval was performed in 10 mM citrate buffer (pH 6.0; anti-human nuclei), 0.5% trypsin (anti-type I, II collagen), or a combination of hyaluronidase (2 mg/mL in PBS) and pronase (1 mg/mL in PBS; anti-type X collagen) [40].

All stained specimens were imaged with an Olympus FSX100 microscope (Tokyo, JP), with the exception of stained rat menisci, which were imaged with an Olympus BX61VS microscope.

## 2.11. Statistical analysis

All statistical analysis was performed using GraphPad Prism (La Jolla, CA;  $\alpha = 0.05$ ): unpaired *t*-tests for decellularization and  $t_{1/2}$ , one-way ANOVA with Tukey *post-hoc* tests for degradation and explant studies, two-way ANOVA (no matching) with Bonferroni *post-hoc* tests for hydrogel studies, paired *t*-tests for percentage tissue regeneration, and two-way ANOVA (matched values from left and right knees per animal) with Bonferroni *post-hoc* tests for animal studies. Data is shown as mean  $\pm$  SEM of biological replicates.

## 3. Results

### 3.1. Study design

We designed three sets of studies to systematically test our hypothesis: (i) tissue development *in vitro* by hMSCs in mECM hydrogel (Figure 1a), (ii) integration of hMSC-mECM hydrogel constructs with meniscal explants *in vitro* (Figure 1b) and *in vivo* (Figure 1c), and (iii) *in situ* injection of hMSCs in mECM hydrogel in an orthotopic nude rat model of meniscal injury (Figure 1d).

### 3.2. Fibrochondrogenesis of hMSCs was superior in mECM hydrogel compared to type I collagen alone, but required growth factor supplementation

hMSCs encapsulated in mECM hydrogel and cultured in the presence of TGF- $\beta$ 3 (mECM+) exhibited greater fibrochondrogenesis than cells in type I collagen (collagen+, Figure 2a). DNA content of collagen hydrogels (+) decreased throughout the 28-day culture period,

while the NA content of mECM hydrogels (+) initially decreased between days 0 and 14, and then was maintained from days 14 to 28.

Sulfated glycosaminoglycan (GAG) and *ortho*-hydroxyproline (OHP, representative of total collagen) content were both significantly higher for mECM than collagen constructs at day 28. OHP content of collagen constructs decreased throughout the culture period, in contrast to mECM constructs, in which it recovered significantly between days 14 and 28. The loss of OHP in hMSC-mECM hydrogel constructs correlated with the depletion of OHP in cultures of acellular hydrogel constructs (Figure S3). In the absence of TGF- $\beta$ 3, neither mECM (-) nor type I collagen (-) hydrogels significantly supported fibrochondrogenesis of hMSCs (Figure 2a), with decreases in cell numbers and OHP content for both hydrogels, and the lack of sulfated GAG production.

Histological analysis was consistent with biochemical contents, demonstrating the production of matrix rich in sulfated GAGs (Alcian blue; Figure 2b) and collagens (Picrosirius red) in mECM constructs cultured with TGF- $\beta$ 3 (+). Cells in mECM hydrogel (+) were situated within well-developed lacunae visualized by H&E staining, which were absent in collagen hydrogel (+).

Expression of key meniscus ECM genes - aggrecan (*ACAN*), the predominant proteoglycan in meniscus, and type II collagen (*COL2A1*) (Figure 3a) was significantly upregulated in hMSC-laden mECM gels with TGF- $\beta$ 3 at day 28, compared to the initial values. In collagen constructs, type I and X collagen were upregulated, suggesting a more fibrous and hypertrophic phenotype.

Correlation of these gene expression patterns to the presence of proteins revealed markedly positive staining for type II collagen in both hMSC-mECM and hMSC-collagen constructs (+) at day 28 (Figure 3b). Collagen I staining was present throughout collagen constructs at day 28, but was limited to the edges of mECM constructs and the cell lacunae, rather than secreted into the newly synthesized ECM. Positive staining for type X collagen appeared in both collagen and mECM constructs, with intracellular staining in collagen constructs, indicative of sustained production, that is not seen in mECM. At day 0, weak but positive staining for type I collagen appears in both constructs, consistent with type I collagen as the basis for gelation of both materials. However, only cells in mECM exhibited positive type II collagen staining, which is present in native meniscus ECM. Finally, no visible staining for type X collagen appeared in either hydrogel at day 0, signifying an absence of type X collagen in juvenile bovine meniscus ECM.

Both mECM and collagen constructs contained high amounts of OHP, but showed weak staining for Picrosirius red and specific collagens. By day 28, OHP content in collagen constructs has decreased, but the staining remained prominent. These differences result from the two distinct methods of collagen determination. OHP quantitation is indicative of total collagen and does not differentiate the fibrillar collagens in hydrogel from mature collagens synthesized by hMSCs [35]. Immunostaining of specific intact epitopes demonstrates the maturation and organization of collagenous proteins after culture with TGF- $\beta$ 3 (Figure 3a,b).

### 3.3. hMSCs in mECM hydrogel enhanced integrative repair of meniscal explants

Delivery of hMSCs in mECM hydrogel into full-thickness defects in meniscal explants significantly improved the integrative strength and biochemical properties of the repair tissue over 42 days of culture (Figure 4a). The increases in biochemical contents in the repair tissue were consistent with the trends observed in hMSC-hydrogel studies.

DNA content decreased between days 0 and 14, and was then maintained for the remainder of culture. Sulfated GAG content increased significantly over 42 days of culture. While total OHP content at day 0 was lower than in hydrogel studies, the trends are consistent: OHP content decreased within the first 14 days of culture due to hydrogel degradation, recovered by day 28 and continued to increase through day 42, due to the synthesis and deposition of new tissue matrix. H&E staining revealed the organization of cells separated by newly synthesized ECM, rich in sulfated GAG (Alcian blue) and collagens (Picrosirius red) (Figure 4b, top panels). In particular, the development of cell lacunae was prominent at the defect interface.

After 42 days *in vitro*, hMSC-mECM constructs were implanted subcutaneously for an additional four weeks. By day 70, well-developed lacunae were seen throughout the constructs, with abundant matrix rich in sulfated GAG and collagens (Figure 4b, bottom panels). Collagen II staining was uniform throughout the mECM gel before implantation, with localized staining at the periphery of cell lacunae in the pericellular matrix. Moreover, the intensity of type I and II collagen staining in the meniscal extracellular matrix and the surrounding explant were comparable (Figure 5). After implantation, this staining remained uniform within the constructs. In contrast, type I collagen staining before implantation was confined to the pericellular matrix, whereas the matrix uniformly stained for type I collagen after *in vivo* culture. Collagen X staining was minimal pre-implantation, and remained low post-implantation, despite staining for mineralization that ranged from negative to moderate (Figure S4). Immunohistochemistry of cell nuclei verified that the cells were of human origin.

### 3.4. hMSCs delivered in mECM into meniscal injury incorporated into host tissue

The *in situ* model of meniscal injury was utilized to further test the *in vivo* performance of mECM hydrogel for meniscal repair. The intra-articular joint space is natively avascular, in contrast to the vascularized subcutaneous environment. We demonstrate the medial parapatellar approach used to access the medial knee joint space and excise the anterior horn of the medial meniscus in our rat model (Figure 6a). Representative images of a whole rat medial meniscus (Figure 6b) and the excised anterior medial meniscal tissue at time of surgery (Figure 6c) are provided for comparison to the gross appearance of control and experimental medial menisci *in situ* (Figure 6d-e) and *ex vivo* (Figure 6f) at 8 weeks after surgery. The percentage resection of medial meniscus by area is approximately  $50.9 \pm 6.0\%$  ( $n = 5$ ) at the time of surgery. The macroscopic appearance of the control medial meniscus at 8 weeks after injury (Figure 6d) suggests minimal to no tissue regeneration. Therefore, we did not quantify the area of regenerated meniscal tissue in control samples. Both medial menisci treated with hMSCs in PBS (Figure 6f) and mECM hydrogel (Figure 6e,f) appear to have regenerated tissue, with the latter appearing to regenerate the most tissue of the three



groups (Figure 6d-f). These observations are supported by the high percentages of regenerated meniscal tissue by area for both groups receiving hMSCs, with a significantly greater percentage tissue regeneration by hMSCs in mECM hydrogel versus PBS (Figure 6g).

We focus on radial cross-sections of meniscal tissue (Figure 7) encompassing the outer and inner regions of the medial meniscus. Across control (Figure 7a,b) and experimental (Figure 7c,d) meniscus, H&E staining reveals cell nuclei distributed throughout the tissue, surrounded by abundant ECM. The extent and quality of this matrix varied in histologic appearance, with dense connective tissue interrupted by mineral deposits (by von Kossa staining) in menisci that did not receive hMSCs delivered in mECM hydrogel (Figure 7a,b,d).

Alcian blue revealed the presence of sulfated GAG in all groups, with weaker staining in the regions of tissue mineralization (Figure 7a,b,d). Picrosirius red staining demonstrated the presence of collagens throughout all menisci, with varying amounts of type I, II and X collagen in the experimental and control groups. Regions of most positive staining for human nuclei correlated with the presence of sulfated GAGs and type II collagen, and low concentrations of type I collagen (Figure 7c,d), which is typical for the inner region of the meniscus that is reminiscent of hyaline cartilage.

The presence of human cell nuclei in both mECM (Figure 7c) and PBS (Figure 7d) menisci indicates the retention and incorporation of exogenous hMSCs to the zone of injury via either delivery vehicle. However, only the experimental tissue that received hMSCs in mECM hydrogel was free of mineralization by von Kossa staining (Figure 7c). Collagen X staining, associated with hypertrophic cartilage, and mineralization was present in all other menisci subjected to injury (Figure 7a,b,d), including tissue that received hMSCs in PBS, suggesting that only exogenous stem cells delivered in mECM hydrogel protected the injured tissue from calcification.

### 3.5. In situ delivery of hMSCs in mECM hydrogel after injury preserved knee joint spaces

Joint space narrowing due to loss of cartilage thickness is a radiographic hallmark of OA, along with subchondral sclerosis and osteophytes [41]. We quantified joint space volumes (JSV) between the distal femur and proximal tibia by three-dimensional (3-D) segmentation of CT images (Figure 8a), as surrogates for joint space narrowing over time after meniscal injury. Calculating JSV by 3-D segmentation allowed for more representative measurements, taking into account the anatomy of the knee [42]. No significant differences were found between JSV of the right versus left control knees at each time point, indicating the reproducibility of the surgical technique. Across all groups, JSV significantly decreased from week 4 to 8, suggesting the loss of cartilage thickness after meniscal injury, regardless of intervention. Knees that received hMSCs in mECM hydrogel [mECM (R)] retained higher JSV than knees that received cells in PBS [PBS (L)] at all imaged time points, suggesting chondroprotective effects of mECM hydrogel (Figure 8b).

## 4. Discussion

Tissue-specific hydrogels can be produced from the extracellular matrix (ECM) of decellularized tissues and utilized in clinical settings either alone or as vehicles for drugs, biologics, or cells to regenerate diseased tissues. We show that a tissue-specific hydrogel derived from decellularized meniscus ECM (mECM) retained characteristic elements of the native tissue guiding the fibrochondrogenesis of human mesenchymal stem cells (hMSCs) and provided the foundation for engineering meniscal repair tissue, both *in vitro* and *in vivo*.

*In vitro* culture of hMSCs in mECM hydrogel exhibited cell growth, sulfated GAG and collagen production superior to cells in type I collagen alone, demonstrating the importance of ECM components. The enhanced fibrochondrogenesis of hMSCs observed in mECM gel suggested its utility for *in situ* delivery of MSCs into full-thickness defects in meniscal explants for integrative repair. hMSCs delivered in mECM hydrogel adhered to meniscal defects and elaborated extensive fibrocartilaginous matrix, culminating in integrative repair *in vitro*. However, these hMSC-mECM explants exhibited variable stability of fibrochondrogenic phenotype and mineralization after an additional four weeks of implantation in a highly vascularized subcutaneous milieu. Limitations exist in translating results in the highly vascularized subcutaneous space to the predominantly avascular intra-articular knee environment. Moreover, while decellularized ECM scaffolds have been produced from a variety of tissues including previously published protocols for meniscus [43–46] and cartilage [47,48], few have been assessed for biological activity at their site of action *in vivo*.

To overcome these limitations, we evaluated the mECM hydrogel as a vehicle for intra-articular delivery of MSCs in an orthotopic rat model of meniscal repair. The rat is among the smallest animal models published in meniscus literature. Inducing meniscal injury is a common method of modeling experimental OA in the rat [49], corroborating long-term studies in human patients, which have shown an association between meniscal tears or extrusion and OA progression [50].

Meniscal tears are often degenerative in patients over 60 years of age, in contrast to younger patients, in which tears are more often traumatic in nature [51–55]. Our findings using the hemi-menisectomy model are more applicable to traumatic injuries in younger patients, emphasizing the importance of preventing joint degradation and OA. Previous studies using Sprague-Dawley rather than athymic nude rats reported near to complete regeneration of injured menisci in tissue area, if not in quality, by 12 weeks in all animals regardless of intervention [29,56]. However, only limited assessments of meniscal tissue hypertrophy and OA development in the joint were published in these studies.

The therapeutic objectives of intra-articular hMSC delivery in mECM hydrogel after meniscal injury in a rat model are to regenerate meniscal tissue and to protect the joint from OA development. At eight weeks post-injury, we demonstrated significant tissue regeneration in menisci that received hMSCs in mECM hydrogel versus PBS. In contrast to prior rat studies [29,56], we observed minimal tissue regeneration in control animals that did not receive hMSCs, which may reflect differences in innate healing between wild-type and

nude rats with compromised immune systems. This finding, together with the persistence of human nuclei staining at end point histological analysis, suggests that tissue regeneration is due to hMSC retention within the knee joint, infiltration and differentiation into a fibrocartilage-like tissue. This regenerated tissue occurred after hMSC delivery in PBS or mECM hydrogel, and exhibited positive staining for markers consistent with meniscal ECM, sulfated GAG, type I and II collagen. However, no mineralization was detected at the eight-week end point only in knees injected with hMSCs in mECM hydrogel, in contrast to the mineralization seen in all other conditions, including hMSCs injected in PBS. It should be noted that calcified matrix is characteristic of native rat meniscus, unlike human meniscus [57]. Nevertheless, injured tissue that received stem cell intervention via mECM hydrogel did not demonstrate histological evidence of mineralization, suggesting mECM hydrogel provided protection from pathologic calcification of this regenerated tissue in addition to tissue regeneration by the exogenous hMSCs. These effects appear to be mediated by the unique combination of mECM hydrogel and hMSCs, and are not secondary to hMSC retention alone as regeneration and mineralization were present in tissues that received hMSCs in PBS. This is significant, as hypertrophy and evidence of terminal differentiation to bone in MSCs has been reported extensively both *in vitro* and *in vivo* [50,58]. In the context of meniscus, increased expression of type X collagen protein has been detected in aged and degenerative OA menisci [59,60], which generally correlated with calcification *in vivo* [61,62].

At the eight-week study end point, we observed the loss of joint space volume (JSV) across all groups, which may reflect the development of post-traumatic OA that is known to follow destabilization of the medial meniscus [63]. However, the JSV in knees that received hMSCs in mECM hydrogel remained significantly greater than in knees that received hMSCs in PBS. Taken together, these two findings, the absence of mineralization and the relative preservation of knee JSV, suggest that the combination of mECM hydrogel and hMSCs promotes the growth of a meniscal-like tissue and chondroprotection of the joint.

Our findings suggest that mECM hydrogel serves two purposes: as an appropriate vehicle to retain MSCs within the intra-articular space, and as a reservoir of native tissue cues to regulate hMSC behavior and formation to fibrocartilage, without hypertrophy or mineralization suggestive of tissue and joint degeneration. The first purpose is to retain sufficient exogenous cells that directly produce new tissue, as demonstrated by the presence of human nuclei and significant tissue regeneration at the study end point. The second purpose is to protect joints from the development of OA, as suggested by the relative maintenance of JSV and absence of mineralization in tissue that received hMSC intervention in mECM hydrogel after meniscal injury. Exogenous stem cells can in turn stimulate endogenous repair cells to produce new tissue. Previous studies have found that the meniscus itself contains a subpopulation of multipotential cells [23,30,36,64], which can be utilized to regenerate tissue. Moreover, the combination of MSCs with native meniscal cells is known to prevent MSC hypertrophy [65,66]. Future work will focus on the interactions between exogenously delivered MSCs and endogenous meniscal cells under the direction of meniscus tissue-specific cues present in mECM hydrogel. The precise identities of these tissue cues remain under investigation, although TGF- $\beta$  has been widely implicated in prior studies of meniscus and articular cartilage. Higher concentrations of TGF- $\beta$  and bFGF have

been detected in growth factor analysis of meniscal ECM [46]. Thrombospondin is a component of the meniscus ECM [67], which contains a specific sequence that activates the latent TGF- $\beta$  complex. Latent TGF- $\beta$  itself is known to be liberated and activated by mechanical shear in devitalized articular cartilage [68]. Additionally, it has been postulated that “matrikine” species derived from the partial proteolysis of ECM proteins [69] regulate cell activity including proliferation and migration. These may all be present in our decellularized ECM hydrogel and account for the marked stem cell differentiation and meniscal tissue formation seen in our studies. Characterizing the key regulators and mechanisms of repair by exogenous hMSCs and activation of endogenous repair cells requires further experimentation, including synovial fluid collection for trophic and inflammatory biomarkers, and data from intermediate time points.

In summary, we present the first report of directed delivery of stem cells into an animal model of meniscal repair, using a hydrogel preparation of decellularized meniscus ECM. Prior studies have reported promising results in meniscal regeneration utilizing meniscus ECM preparations in allograft [16,20,70], hydrogel [43,44], and soluble [46] forms; MSCs derived from the bone marrow [71–73], synovium [29], and meniscus [23,31]; and evaluation in animal models ranging from subcutaneous implantation [43,45] to intra-articular injections in rats [29,31,72] up to primates [74]; but none have studied the combination of MSCs and meniscus ECM hydrogel at their relevant site of action. We demonstrate the use of decellularized bovine meniscus hydrogel for intra-articular delivery of human mesenchymal stem cells in an orthotopic nude rat model of meniscal injury. Our hydrogel provided a foundation for stem cell-based repair, via preservation and presentation of biological cues from the native tissue environment, resulting in elaboration of fibrocartilaginous tissue matrix *in vivo*. Evaluation of mECM hydrogel *in situ* in a rat model of meniscal injury demonstrated the contribution of mECM towards meniscal regeneration and integration with host tissue, and suggested chondroprotection within the joint. Our conclusions are limited by the absence of a non-tissue-specific vehicle for hMSCs in the rat model of meniscal injury. We chose PBS as a control vehicle for comparison to past rat studies in which PBS was utilized as the experimental vehicle for MSCs [29,72,75]. In future work with a larger number of rats or in a larger animal model such as rabbit [14] or sheep [76], our mECM hydrogel can be compared with a non-meniscus-specific ECM carrier, such as dehydrated amniotic tissue [77], or a single ECM component such as type I collagen.

Further animal work will also benefit from correlating histologic and radiologic biomarkers of repair in longitudinal studies for improving prediction of clinical outcomes while decreasing reliance on tissue sampling for histology. Radiologic monitoring such as non-invasive bioluminescence imaging to monitor cell retention *in vivo* and MRI imaging to track soft tissue changes and OA development [51,52] are more practical, conservative, and clinically applicable means of assessing joint changes. Interpretation of our imaging results is limited by the absence of baseline JSV, due to a malfunctioning x-ray tube requiring replacement. We were only able to obtain imaging data starting from week 4 and cannot report the loss of JSV over the first four weeks post-injury. In addition, the indirect calculation of JSV may be affected by large joint effusions masquerading as larger JSV, or joint contractures compressing the femur and tibia together and yielding effectively smaller

JSV. Histological evaluation of the knee joint cartilage to document joint degeneration is a means of providing direct evidence of chondroprotection rather than indirect measurements of JSV alone.

Currently, we are focusing on hydrogel development by modifying mechanical and viscoelastic properties of the mECM hydrogel, such as by *in situ* crosslinking, in order to improve cell and hydrogel retention within the intra-articular space, and translating this technology to other musculoskeletal diseases, including OA, tendinopathies, and injuries to other fibrocartilaginous tissues.

## Supplementary Material

Refer to Web version on PubMed Central for supplementary material.

## Acknowledgments

We thank Dr. Donald Freytes and John O'Neill for sharing their expertise for decellularization of meniscal tissues and preparation of ECM-derived hydrogels; Dr. Supansa Yodmuang for her help with protein analysis; Susan Halligan for her assistance with subcutaneous implantations; Dr. Christopher Ahmad for his clinical insight into meniscal pathology; and Dr. Lynne Johnson and Tamykah Anthony for their work with animal imaging. The work was funded by NIH (grants DE016525, EB002520, and AR061988).

## References

1. Singelyn JM, DeQuach JA, Seif-Naraghi SB, Littlefield RB, Schup-Magoffin PJ, Christman KL. Naturally derived myocardial matrix as an injectable scaffold for cardiac tissue engineering. *Biomaterials*. 2009; 30:5409–16. [PubMed: 19608268]
2. Petersen TH, Calle EA, Zhao L, Lee EJ, Gui L, Raredon MB, et al. Tissue-Engineered Lungs for *in Vivo* Implantation. *Science* (80-). 2010; 329:538–41.
3. Grayson WL, Fröhlich M, Yeager K, Bhumiratana S, Chan ME, Cannizzaro C, et al. Engineering anatomically shaped human bone grafts. *Proc Natl Acad Sci U S A*. 2010; 107:3299–304. [PubMed: 19820164]
4. Freytes DO, Martin J, Velankar SS, Lee AS, Badylak SF. Preparation and rheological characterization of a gel form of the porcine urinary bladder matrix. *Biomaterials*. 2008; 29:1630–7. [PubMed: 18201760]
5. Badylak SF. The extracellular matrix as a biologic scaffold material. *Biomaterials*. 2007; 28:3587–93. [PubMed: 17524477]
6. Freymann U, Metzclaff S, Krüger JP, Hirsh G, Endres M, Petersen W, et al. Effect of Human Serum and 2 Different Types of Platelet Concentrates on Human Meniscus Cell Migration, Proliferation, and Matrix Formation. *Arthrosc J Arthrosc Relat Surg*. 2016; 32:1106–16.
7. Strauss EJ, Hart JA, Miller MD, Altman RD, Rosen JE. Hyaluronic Acid Viscosupplementation and Osteoarthritis. *Am J Sports Med*. 2009; 37:1636–44. [PubMed: 19168804]
8. Foster TE, Puskas BL, Mandelbaum BR, Gerhardt MB, Rodeo SA. Platelet-Rich Plasma: From Basic Science to Clinical Applications. *Am J Sports Med*. 2009; 37:2259–72. [PubMed: 19875361]
9. Rodkey WG, Steadman JR, Li ST. A clinical study of collagen meniscus implants to restore the injured meniscus. *Clin Orthop Relat Res*. 1999:S281–92. [PubMed: 10546653]
10. Higuchi H, Kimura M, Shirakura K, Terauchi M, Takagishi K. Factors affecting long-term results after arthroscopic partial meniscectomy. *Clin Orthop Relat Res*. 2000; 377:161–8.
11. Wirth CJ, Peters G, Milachowski KA, Weismeier KG, Kohn D. Long-term results of meniscal allograft transplantation. *Am J Sports Med*. 2002; 30:174–81. [PubMed: 11912084]
12. Stone KR, Steadman JR, Rodkey WG, Li ST. Regeneration of meniscal cartilage with use of a collagen scaffold. Analysis of preliminary data *J Bone Joint Surg Am*. 1997; 79:1770–7. [PubMed: 9409790]

13. Zhang ZZ, Jiang D, Wang SJ, Qi YS, Ding JX, Yu JK, et al. Scaffolds drive meniscus tissue engineering. *RSC Adv.* 2015; 5:77851–9.
14. Zhang ZZ, Jiang D, Ding JX, Wang SJ, Zhang L, Zhang JY, et al. Role of scaffold mean pore size in meniscus regeneration. *Acta Biomater.* 2016; 43:314–26. [PubMed: 27481291]
15. Stapleton TW, Ingram J, Katta J, Knight R, Korossis S, Fisher J, et al. Development and characterization of an acellular porcine medial meniscus for use in tissue engineering. *Tissue Eng Part A.* 2008; 14:505–18. [PubMed: 18370607]
16. Sandmann GH, Eichhorn S, Vogt S, Adamczyk C, Aryee S, Hoberg M, et al. Generation and characterization of a human acellular meniscus scaffold for tissue engineering. *J Biomed Mater Res - Part A.* 2009; 91:567–74.
17. Stabile KJ, Odom D, Smith TL, Northam C, Whitlock PW, Smith BP, et al. An Acellular, Allograft-Derived Meniscus Scaffold in an Ovine Model. *Arthrosc - J Arthrosc Relat Surg.* 2010; 26:936–48.
18. Minehara H, Urabe K, Naruse K, Mehlhorn AT, Uchida K, Südkamp NP, et al. A new technique for seeding chondrocytes onto solvent-preserved human meniscus using the chemokinetic effect of recombinant human bone morphogenetic protein-2. *Cell Tissue Bank.* 2011; 12:199–207. [PubMed: 20556521]
19. Arnoczky SP, DiCarlo EF, O'Brien SJ, Warren RF. Cellular repopulation of deep-frozen meniscal autografts: an experimental study in the dog. *Arthroscopy.* 1992; 8:428–36. [PubMed: 1466700]
20. Stapleton TW, Ingram J, Fisher J, Ingham E. Investigation of the regenerative capacity of an acellular porcine medial meniscus for tissue engineering applications. *Tissue Eng Part A.* 2011; 17:231–42. [PubMed: 20695759]
21. Buma P, Ramrattan NN, Van Tienen TG, Veth RPH. Tissue engineering of the meniscus. *Biomaterials.* 2004; 25:1523–32. [PubMed: 14697855]
22. Barry F, Murphy M. Mesenchymal stem cells in joint disease and repair. *Nat Rev Rheumatol.* 2013; 9:1–11. [PubMed: 23229451]
23. Ding Z, Huang H. Mesenchymal stem cells in rabbit meniscus and bone marrow exhibit a similar feature but a heterogeneous multi-differentiation potential: superiority of meniscus as a cell source for meniscus repair. *BMC Musculoskelet Disord.* 2015; 16:65. [PubMed: 25887689]
24. Centeno CJ, Busse D, Kisiday J, Keohan C, Freeman M, Karli D. Regeneration of meniscus cartilage in a knee treated with percutaneously implanted autologous mesenchymal stem cells. *Med Hypotheses.* 2008; 71:900–8. [PubMed: 18786777]
25. Centeno CJ, Al-Sayegh H, Freeman MD, Smith J, Murrell WD, Bubnov R. A multi-center analysis of adverse events among two thousand, three hundred and seventy two adult patients undergoing adult autologous stem cell therapy for orthopaedic conditions. *Int Orthop.* 2016; 40:1755–65. [PubMed: 27026621]
26. Murphy JM, Fink DJ, Hunziker EB, Barry FP. Stem cell therapy in a caprine model of osteoarthritis. *Arthritis Rheum.* 2003; 48:3464–74. [PubMed: 14673997]
27. Silverman RP, Passaretti D, Huang W, Randolph MA, Yaremchuk MJ. Injectable tissue-engineered cartilage using a fibrin glue polymer. *Plast Reconstr Surg.* 1999; 103:1809–18. [PubMed: 10359239]
28. Radice M, Brun P, Cortivo R, Scapinelli R, Battaliard C, Abatangelo G. Hyaluronan-based biopolymers as delivery vehicles for bone-marrow-derived mesenchymal progenitors. *J Biomed Mater Res.* 2000; 50:101–9. [PubMed: 10679672]
29. Horie M, Sekiya I, Muneta T, Ichinose S, Matsumoto K, Saito H, et al. Intra-articular Injected synovial stem cells differentiate into meniscal cells directly and promote meniscal regeneration without mobilization to distant organs in rat massive meniscal defect. *Stem Cells.* 2009; 27:878–87. [PubMed: 19350690]
30. Shen W, Chen J, Zhu T, Yin Z, Chen X, Chen L, et al. Osteoarthritis prevention through meniscal regeneration induced by intra-articular injection of meniscus stem cells. *Stem Cells Dev.* 2013; 22:2071–82. [PubMed: 23461527]
31. Shen W, Chen J, Zhu T, Chen L, Zhang W, Fang Z, et al. Intra-Articular Injection of Human Meniscus Stem/Progenitor Cells Promotes Meniscus Regeneration and Ameliorates Osteoarthritis

- Through Stromal Cell-Derived Factor-1/CXCR4-Mediated Homing. *Stem Cells Transl Med.* 2014; 3:387–94. [PubMed: 24448516]
32. Centeno CJ, Busse D, Kisiday J, Keohan C, Freeman M, Karli D. Increased Knee Cartilage Volume in Degenerative Joint Disease using Percutaneously Implanted. Autologous Mesenchymal Stem Cells. 2008; i:343–53.
  33. Vangsness T, Farr J, Boyd J, Dellaero DT, Mills CR, Leroux-Williams M. Adult Human Mesenchymal Stem Cells Delivered via Intra-Articular Injection to the Knee Following Partial Medial Meniscectomy. *J Bone Jt Surg.* 2014; 96:90–8.
  34. Peeters CMM, Leijns MJC, Reijman M, van Osch GJVM, Bos PK. Safety of intra-articular cell-therapy with culture-expanded stem cells in humans: A systematic literature review. *Osteoarthr Cartil.* 2013; 21:1465–73. [PubMed: 23831631]
  35. Reddy GK, Enwemeka CS. A simplified method for the analysis of hydroxyproline in biological tissues. *Clin Biochem.* 1996; 29:225–9. [PubMed: 8740508]
  36. Mauck RL, Martinez-Diaz GJ, Yuan X, Tuan RS. Regional multilineage differentiation potential of meniscal fibrochondrocytes: Implications for meniscus repair. *Anat Rec.* 2007; 290:48–58.
  37. Tognana E, Chen F, Padera RF, Leddy HA, Christensen SE, Guilak F, et al. Adjacent tissues (cartilage, bone) affect the functional integration of engineered calf cartilage in vitro. *Osteoarthr Cartil.* 2005; 13:129–38. [PubMed: 15694574]
  38. Obradovic B, Martin I, Padera RF, Treppo S, Freed LE, Vunjak-Novakovic G. Integration of engineered cartilage. *J Orthop Res.* 2001; 19:1089–97. [PubMed: 11781010]
  39. Farndale RW, Buttle DJ, Barrett AJ. Improved quantitation and discrimination of sulphated glycosaminoglycans by use of dimethylmethylene blue. *Biochim Biophys Acta.* 1986; 883:173–7. [PubMed: 3091074]
  40. Aigner T, Gresk-otter KR, Fairbank JC, von der Mark K, Urban JP. Variation with age in the pattern of type X collagen expression in normal and scoliotic human intervertebral discs. *Calcif Tissue Int.* 1998; 63:263–8. [PubMed: 9701632]
  41. Altman RD, Gold GE. Atlas of individual radiographic features in osteoarthritis, revised. *Osteoarthr Cartil.* 2007; 15:1–56. [PubMed: 16891130]
  42. Cicuttini F, Hankin J, Jones G, Wluka A. Comparison of conventional standing knee radiographs and magnetic resonance imaging in assessing progression of tibiofemoral joint osteoarthritis. *Osteoarthr Cartil.* 2005; 13:722–7. [PubMed: 15922634]
  43. Wu J, Ding Q, Dutta A, Wang Y, Huang YHH, Weng H, et al. An injectable extracellular matrix derived hydrogel for meniscus repair and regeneration. *Acta Biomater.* 2015; 16:49–59. [PubMed: 25644450]
  44. Visser J, Levett PA, te Moller NCR, Besems J, Boere KWM, van Rijen MHP, et al. Crosslinkable hydrogels derived from cartilage, meniscus, and tendon tissue. *Tissue Eng Part A.* 2015; 21:1195–206. [PubMed: 25557049]
  45. Chen YC, Chen RN, Jhan HJ, Liu DZ, Ho HO, Mao Y, et al. Development and characterization of acellular extracellular matrix scaffolds from porcine menisci for use in cartilage tissue engineering. *Tissue Eng Part C Methods.* 2015; 21:971–86. [PubMed: 25919905]
  46. Rothrauff BB, Shimomura K, Gottardi R, Alexander PG, Tuan RS, Peter G, et al. Anatomical region-dependent enhancement of 3-dimensional chondrogenic differentiation of human mesenchymal stem cells by soluble meniscus extracellular matrix. *Acta Biomater.* 2016; 49:140–51. [PubMed: 27876676]
  47. Yang Q, Peng J, Guo Q, Huang J, Zhang L, Yao J, et al. A cartilage ECM-derived 3-D porous acellular matrix scaffold for in vivo cartilage tissue engineering with PKH26-labeled chondrogenic bone marrow-derived mesenchymal stem cells. *Biomaterials.* 2008; 29:2378–87. [PubMed: 18313139]
  48. Cheng NC, Estes BT, Awad Ha, Guilak F. Chondrogenic differentiation of adipose-derived adult stem cells by a porous scaffold derived from native articular cartilage extracellular matrix. *Tissue Eng Part A.* 2009; 15:231–41. [PubMed: 18950290]
  49. Miller RE, Tran PB, Das R, Ghoreishi-Haack N, Ren D, Miller RJ, et al. CCR2 chemokine receptor signaling mediates pain in experimental osteoarthritis. *Pnas.* 2012; 109:2–7.

50. Johnstone B, Hering TM, Caplan AI, Goldberg VM, Yoo JU. In vitro chondrogenesis of bone marrow-derived mesenchymal progenitor cells. *Exp Cell Res.* 1998; 238:265–72. [PubMed: 9457080]
51. Hunter DJ, Le Graverand MPH, Eckstein F. Radiologic markers of osteoarthritis progression. *Curr Opin Rheumatol.* 2009; 21:110–7. [PubMed: 19339920]
52. Chan KKW, Sit RWS, Wu RWK, Ngai AHY. Clinical, radiological and ultrasonographic findings related to knee pain in osteoarthritis. *PLoS One.* 2014; 9:1–6.
53. Evans CH, Kraus VB, Setton LA. Progress in intra-articular therapy. *Nat Rev Rheumatol.* 2014; 10:11–22. [PubMed: 24189839]
54. Marx RE, Carlson ER, Eichstaedt RM, Schimmele SR, Strauss JE, Georgeff KR. Platelet-rich plasma: Growth factor enhancement for bone grafts. *Oral Surg Oral Med Oral Pathol Oral Radiol Endod.* 1998; 85:638–46. [PubMed: 9638695]
55. Filardo G, Kon E, Buda R, Timoncini A, Di Martino A, Cenacchi A, et al. Platelet-rich plasma intra-articular knee injections for the treatment of degenerative cartilage lesions and osteoarthritis. *Knee Surg Sports Traumatol Arthrosc.* 2011; 19:528–35. [PubMed: 20740273]
56. Katagiri H, Muneta T, Tsuji K, Horie M, Koga H, Ozeki N, et al. Transplantation of aggregates of synovial mesenchymal stem cells regenerates meniscus more effectively in a rat massive meniscal defect. *Biochem Biophys Res Commun.* 2013; 435:603–9. [PubMed: 23685144]
57. Vailas AC, Zernicke RF, Matsuda J, Peller D. Regional biochemical and morphological characteristics of rat knee meniscus. *Comp Biochem Physiol -- Part B Biochem.* 1985; 82:283–5.
58. Pelttari K, Winter A, Steck E, Goetzke K, Hennig T, Ochs BG, et al. Premature induction of hypertrophy during in vitro chondrogenesis of human mesenchymal stem cells correlates with calcification and vascular invasion after ectopic transplantation in SCID mice. *Arthritis Rheum.* 2006; 54:3254–66. [PubMed: 17009260]
59. Eerola I, Salminen H, Lammi P, Lammi M, Von Der Mark K, Vuorio E, et al. Type X collagen, a natural component of mouse articular cartilage: Association with growth, aging, and osteoarthritis. *Arthritis Rheum.* 1998; 41:1287–95. [PubMed: 9663487]
60. Bluteau G, Labourdette L, Ronzière MC, Conrozier T, Mathieu P, Herbage D, et al. Type X collagen in rabbit and human meniscus. *Osteoarthr Cartil.* 1999; 7:498–501. [PubMed: 10489323]
61. Gao J. Immunolocalization of types I, II, and X collagen in the tibial insertion sites of the medial meniscus. *Knee Surg Sports Traumatol Arthrosc.* 2000; 8:61–5. [PubMed: 10663323]
62. Le Graverand MPH, Sciore P, Eggerer J, Rattner JP, Vignon E, Barclay L, et al. Formation and phenotype of cell clusters in osteoarthritic meniscus. *Arthritis Rheum.* 2001; 44:1808–18. [PubMed: 11508433]
63. Culley KL, Dragomir CL, Chang J, Wondimu EB, Coico J, Plumb DA, et al. Mouse models of osteoarthritis: surgical model of posttraumatic osteoarthritis induced by destabilization of the medial meniscus. *Methods Mol Biol.* 2015; 1226:143–73. [PubMed: 25331049]
64. Pedrozo HA, Schwartz Z, Gomez R, Ornoy A, Xin-Sheng W, Dallas SL, et al. Growth plate chondrocytes store latent transforming growth factor (TGF)-beta 1 in their matrix through latent TGF-beta 1 binding protein-1. *J Cell Physiol.* 1998; 177:343–54. [PubMed: 9766531]
65. Cui X, Hasegawa A, Lotz M, D'Lima D. Structured three-dimensional co-culture of mesenchymal stem cells with meniscus cells promotes meniscal phenotype without hypertrophy. *Biotechnol Bioeng.* 2012; 109:2369–80. [PubMed: 22422555]
66. Matthies NF, Mulet-Sierra A, Jomha NM, Adesida AB. Matrix formation is enhanced in co-cultures of human meniscus cells with bone marrow stromal cells. *J Tissue Eng Regen Med.* 2012
67. Miller RR, McDevitt CA. Thrombospondin in ligament, meniscus and intervertebral disc. *BBA - Gen Subj.* 1991; 1115:85–8.
68. Albro MB, Cigan AD, Nims RJ, Yeroushalmi KJ, Oungouljian SR, Hung CT, et al. Shearing of synovial fluid activates latent TGF-β. *Osteoarthr Cartil.* 2012; 20:1374–82. [PubMed: 22858668]
69. Maquart FX, Bellon G, Pasco S, Monboisse JC. Matrikines in the regulation of extracellular matrix degradation. 2005; 87:353–60.
70. Yamasaki T, Deie M, Shinomiya R, Yasunaga Y, Yanada S, Ochi M. Transplantation of meniscus regenerated by tissue engineering with a scaffold derived from a rat meniscus and mesenchymal stromal cells derived from rat bone marrow. *Artif Organs.* 2008; 32:519–24. [PubMed: 18638305]



71. Izuta Y, Ochi M, Adachi N, Deie M, Yamasaki T, Shinomiya R. Meniscal repair using bone marrow-derived mesenchymal stem cells: Experimental study using green fluorescent protein transgenic rats. *Knee*. 2005; 12:217–23. [PubMed: 15911296]
72. Horie M, Choi H, Lee RH, Reger RL, Ylostalo J, Muneta T, et al. Intra-articular injection of human mesenchymal stem cells (MSCs) promote rat meniscal regeneration by being activated to express Indian hedgehog that enhances expression of type II collagen. *Osteoarthr Cartil*. 2012; 20:1197–207. [PubMed: 22750747]
73. Chen, QiY, Feng, GG. Osteoarthritis prevention and meniscus regeneration induced by transplantation of mesenchymal stem cell sheet in a rat meniscal defect model. *Exp Ther Med*. 2016:95–100. [PubMed: 27347022]
74. Kondo S, Muneta T, Nakagawa Y, Koga H, Watanabe T, Tsuji K, et al. Transplantation of autologous synovial mesenchymal stem cells promotes meniscus regeneration in aged primates. *J Orthop Res*. 2016
75. Okuno M, Muneta T, Koga H, Ozeki N, Nakagawa Y, Tsuji K, et al. Meniscus regeneration by syngeneic, minor mismatched, and major mismatched transplantation of synovial mesenchymal stem cells in a rat model. *J Orthop Res*. 2014; 32:928–36. [PubMed: 24644154]
76. Qu F, Pintauro MP, Haughan JE, Henning EA, Esterhai JL, Schaer TP, et al. Repair of dense connective tissues via biomaterial-mediated matrix reprogramming of the wound interface. *Biomaterials*. 2015; 39:85–94. [PubMed: 25477175]
77. Willett NJ, Thote T, Lin ASP, Moran S, Raji Y, Sridaran S, et al. Intra-articular injection of micronized dehydrated human amnion/chorion membrane attenuates osteoarthritis development. *Arthritis Res Ther*. 2014; 16:R47. [PubMed: 24499554]

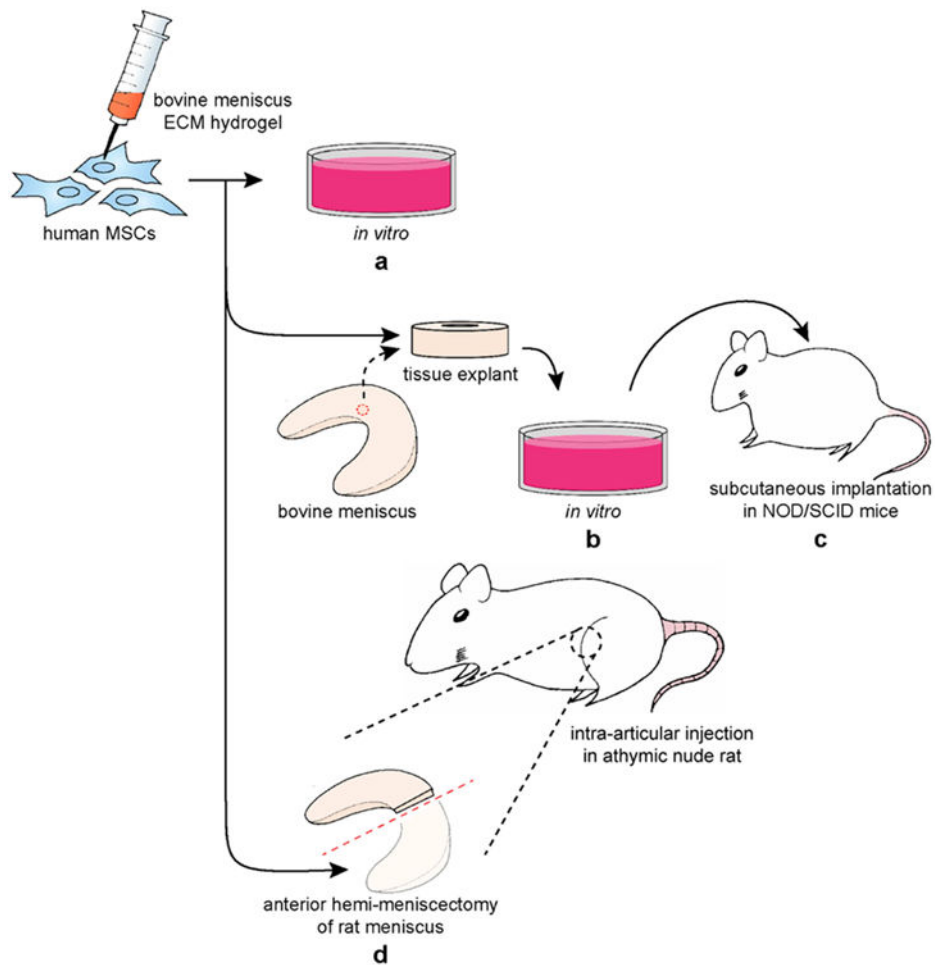


**Figure 1. Schematic of *in vitro* and *in vivo* meniscus ECM experiments**

(a) Comparison of hMSC fibrochondrogenesis in mECM versus type I collagen hydrogels over 28 days *in vitro*. (b) Integration of hMSCs in mECM hydrogel within full-thickness defects in tissue explants harvested from bovine menisci, cultured for 42 days *in vitro*, (c) then implanted subcutaneously in NOD/SCID nude mice for 28 days *in vivo*. (d) Intra-articular delivery of hMSCs in mECM hydrogel by injection into an athymic nude rat model of anterior hemi-menisectomy with analysis up to 8 weeks post-injury *in vivo*.

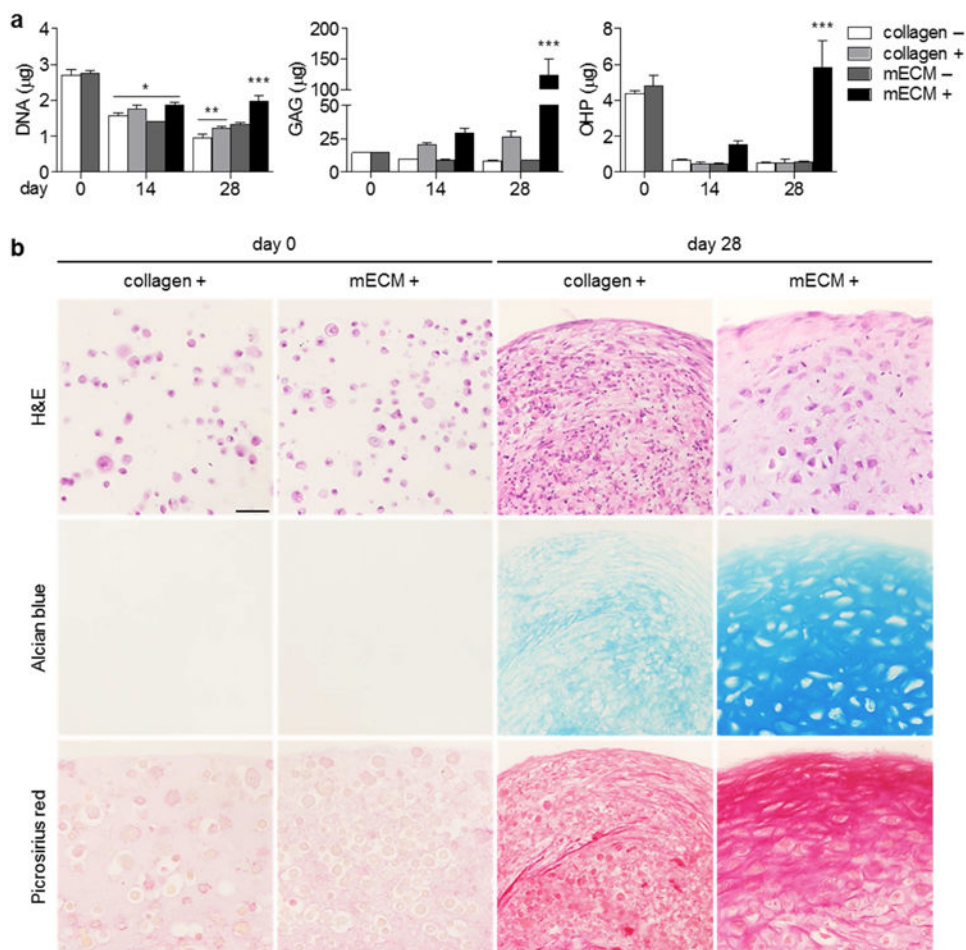


**Figure 2. *In vitro* fibrochondrogenesis of hMSCs in mECM versus type I collagen hydrogels** (a) Culture of hMSCs in mECM and type I collagen hydrogels, with (+) and without (-) 10 ng/mL TGF- $\beta$ 3 over 28 days *in vitro*. Although hMSCs did not differentiate in either hydrogel in the absence of TGF- $\beta$ 3, the cells produced significant matrix in mECM hydrogel with TGF- $\beta$ 3 supplementation. \*  $p < 0.05$  vs. day 0; \*\*  $p < 0.05$  vs. day 14 collagen -, collagen +; \*\*\*  $p < 0.05$  vs. day 28 collagen +, mECM -;  $n = 3-10$ . (b) Histological staining of mECM and type I collagen constructs with TGF- $\beta$ 3 supplementation. hMSCs in mECM hydrogel were arranged in lacunae surrounded by matrix rich in sulfated GAG and collagens, compared to cells in collagen hydrogel. Scale bar: 50  $\mu$ m.

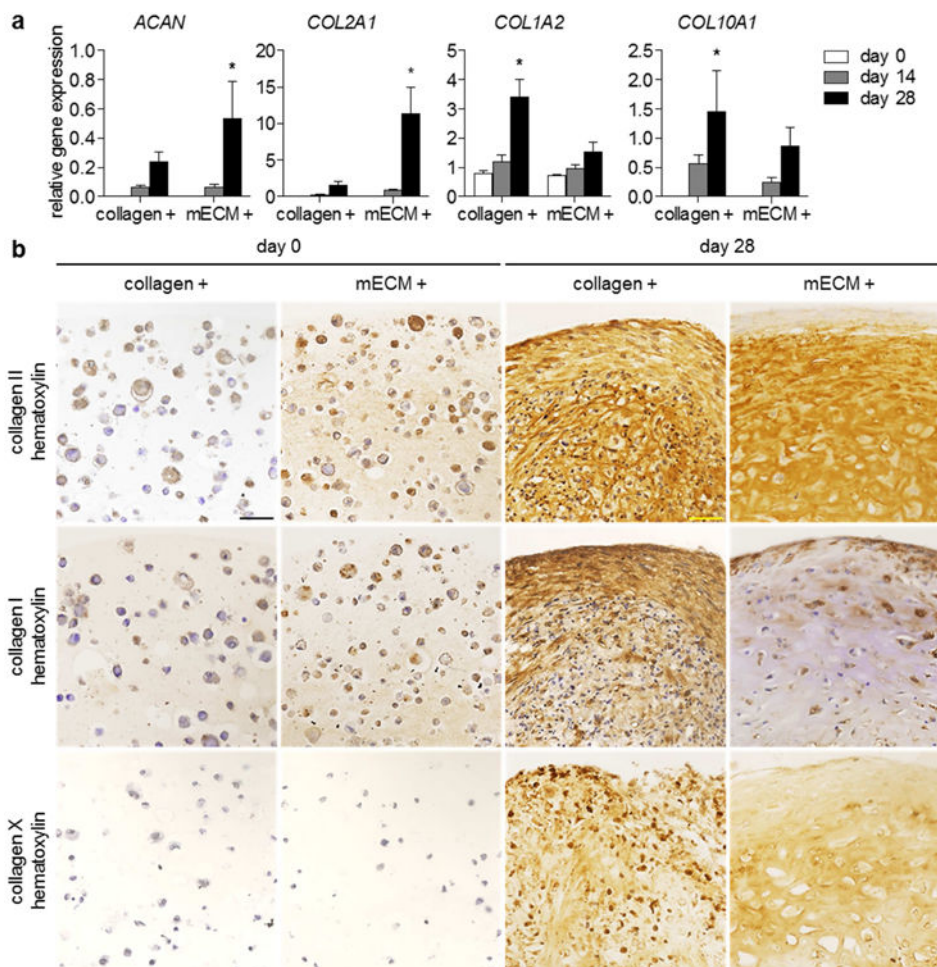


**Figure 3. *In vitro* expression of specific meniscus ECM components in hMSC constructs**  
**(a)** Relative gene expression ( $2^{-C_T}$ ) of hMSCs encapsulated in type I collagen or mECM hydrogels, over 28 days of culture with TGF- $\beta$ 3 supplementation. Expression of aggrecan (*ACAN*) and type II collagen (*COL2A1*) were significantly greater at day 28 in mECM constructs, whereas type I collagen (*COL1A2*) and X (*COL10A1*) were significantly greater at day 28 in collagen constructs. *ACAN*: \*  $p < 0.05$  vs. mECM days 0, 14;  $n = 4$ . *COL2A1*: \*  $p < 0.05$  vs. mECM days 0, 14, collagen day 28;  $n = 4$ . *COL1A2*: \*  $p < 0.05$  vs. collagen days 0, 14, mECM day 28;  $n = 4$ . *COL10A1*: \*  $p < 0.05$  vs. collagen day 0;  $n = 4$ . **(b)** Immunohistochemistry of hMSC-mECM and collagen constructs. Intense staining for type II collagen appears at day 28 in both constructs, but only mECM hydrogel contained type II collagen initially. Positive staining for type I collagen is present in both collagen and mECM constructs at day 0, but staining is more prevalent at day 28 throughout collagen constructs. Collagen X does not appear in either hydrogel at day 0, but develops by day 28, although positive staining is present both intra- and extracellularly. Scale bar: 50  $\mu$ m.

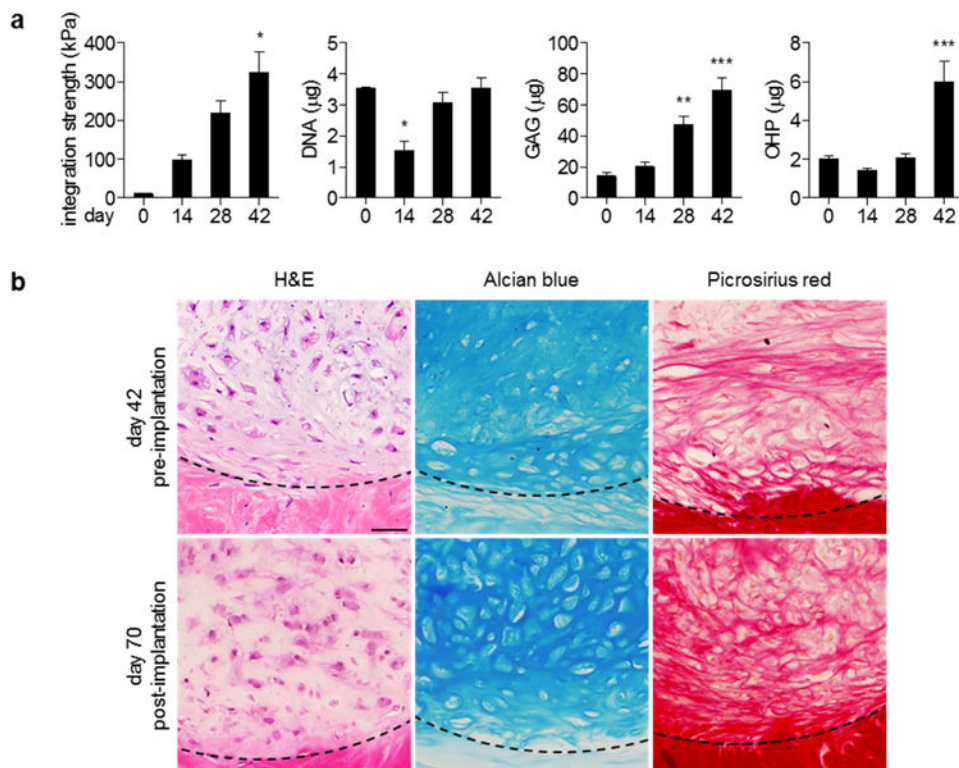


**Figure 4. hMSCs delivered in mECM hydrogel adhere to full-thickness defects in meniscal explants**

(a) Integration strength and biochemical content of hMSC-mECM explants over six weeks *in vitro*. The development of integration strength correlated with significant production of sulfated GAG and collagen. Integration strength: \*  $p < 0.05$  vs. days 0, 14;  $n = 3-8$ . DNA, GAG, OHP: \*  $p < 0.05$  vs. days 0, 28, 42; \*\*  $p < 0.05$  vs. days 0, 14; \*\*\*  $p < 0.05$  vs. days 0, 14, 28;  $n = 3-8$ . (b) Representative images of explants before and after four weeks of *in vivo* subcutaneous implantation. Well-developed lacunae appear throughout the sample, whereas those before implantation are confined at the defect interface, indicated by dashed lines. Scale bar: 50  $\mu\text{m}$ .

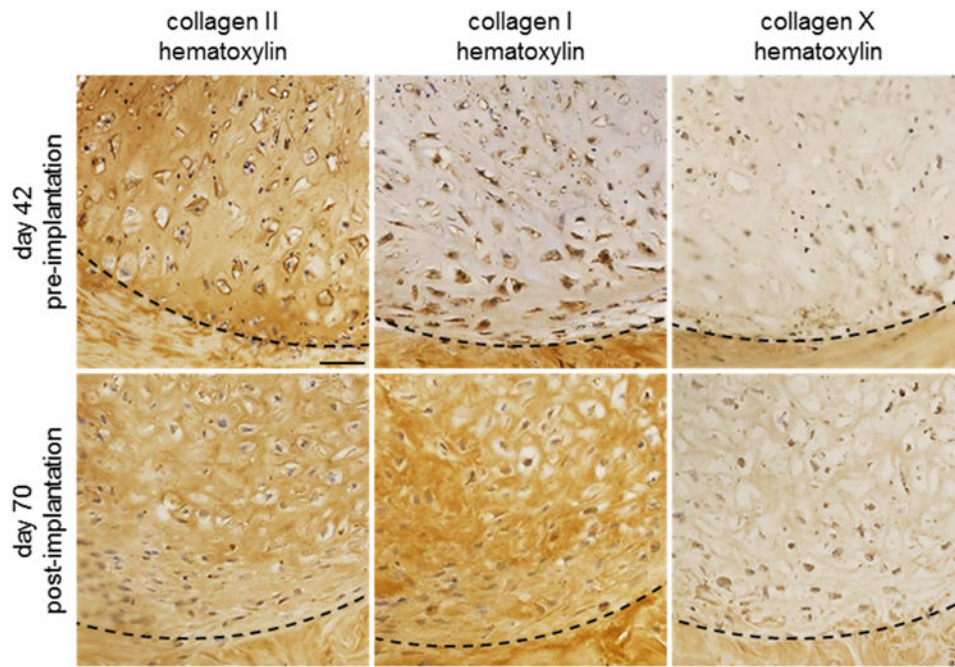


**Figure 5. Expression of fibrochondrogenic and hypertrophic collagens before and after *in vivo* implantation**

After 42 days *in vitro* (pre-implantation), hMSC-mECM explants exhibited intense staining for type II collagen, but not type I collagen or X. After four weeks of implantation (post-implantation), explants were type II and I collagen-positive, but remained largely type X collagen-negative. Dashed lines indicate the defect interface. Scale bar: 50  $\mu\text{m}$ .

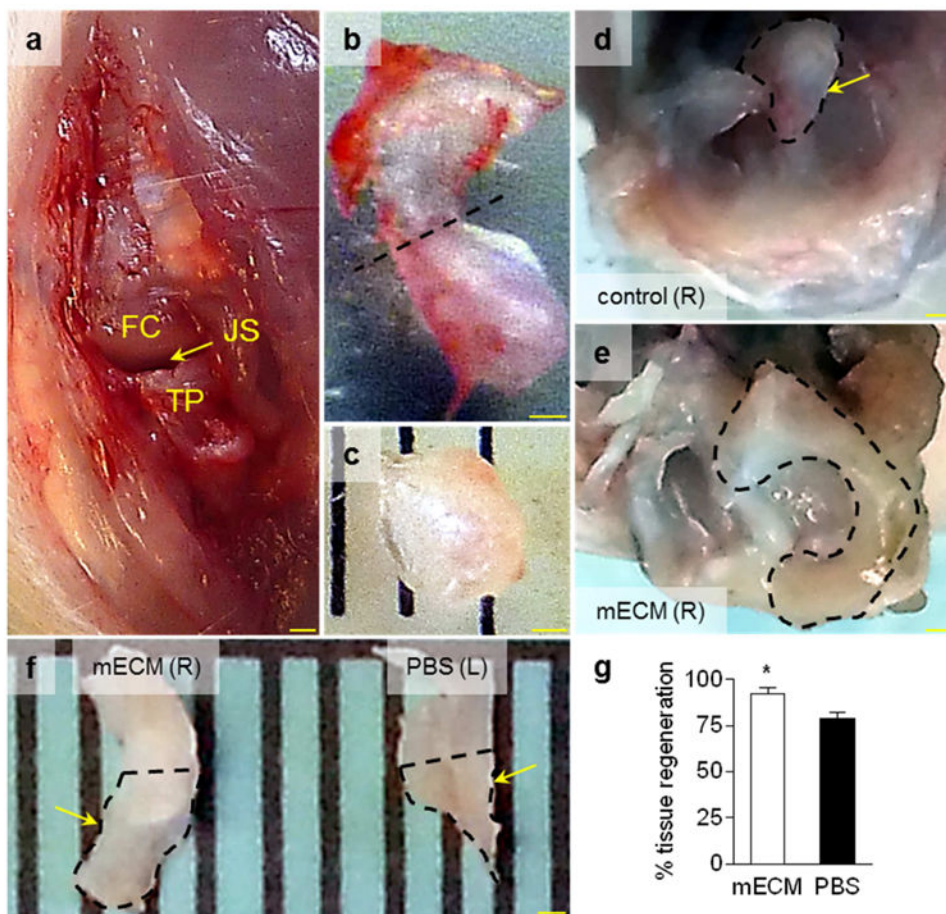


**Figure 6. Macroscopic images of the rat model of meniscal injury and tissues at 8 weeks after injury**

(a) Medial parapatellar approach to access the medial knee joint space (JS) between the medial femoral condyle (FC) and tibial plateau (TP) and excise the anterior horn of the medial meniscus. Representative images of (b) a whole rat medial meniscus and (c) excised meniscal tissue. Dashed line (b) indicates radial cut for tissue excision. (d-f) Meniscal tissues at 8 weeks after injury *in situ* atop the tibial plateau (d-e) and excised from the joint space (f). Representative images of control meniscal tissue that did not receive cells [control (R)] and (d) experimental tissue that received cells in mECM hydrogel [mECM (R)] *in situ*, and (f) tissues that received cells in mECM hydrogel [mECM (R)] or PBS [PBS (L)] *ex vivo*. Dashed lines indicate borders of medial meniscus (d,e) and borders of regenerated meniscal tissue (f). Arrows indicate radial cuts for histology (d,f). (g) Menisci that received cells in mECM hydrogel and PBS both regenerated tissue, although the percentage tissue regeneration (%) by area was significantly greater in menisci that received cells in mECM hydrogel (mECM) than in PBS.  $n = 7$ . \*  $p < 0.05$  vs. PBS. Scale bar: 1 mm (a), 500  $\mu\text{m}$  (b-f).

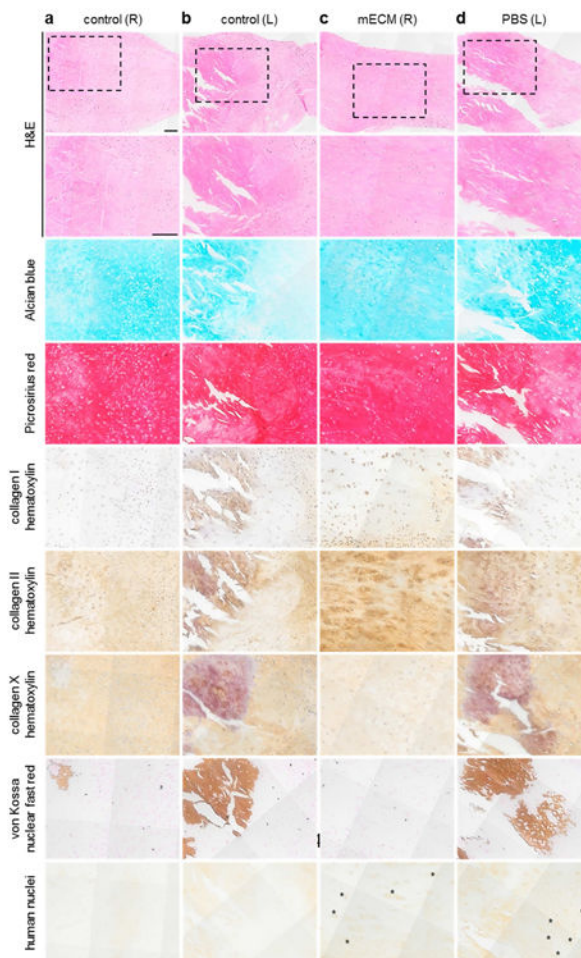


**Figure 7. Cells and extracellular matrix composition of rat menisci at 8 weeks after injury *in vivo*** Representative images of medial menisci in radial cross-sectional views from the bilateral knees of a control animal (**a,b**), which received no cells, and an experimental animal (**c,d**), which received hMSCs delivered in mECM hydrogel ([mECM (R)]; **c**) or in PBS ([PBS (L)]; **d**) at low-power (top row) and high-power magnification (all remaining rows), demonstrating the composition of regenerated tissue at 8 weeks post-injury, notable for retention of cells of human origin under experimental conditions (human nuclei; **c,d**); and mineralization in control menisci without cells (von Kossa; **a,b**), and experimental menisci without mECM hydrogel (von Kossa; **d**). Dashed boxes indicate areas of high-power magnification. Asterisks indicate areas of positive staining for human nuclei. Scale bar: 100  $\mu\text{m}$ .



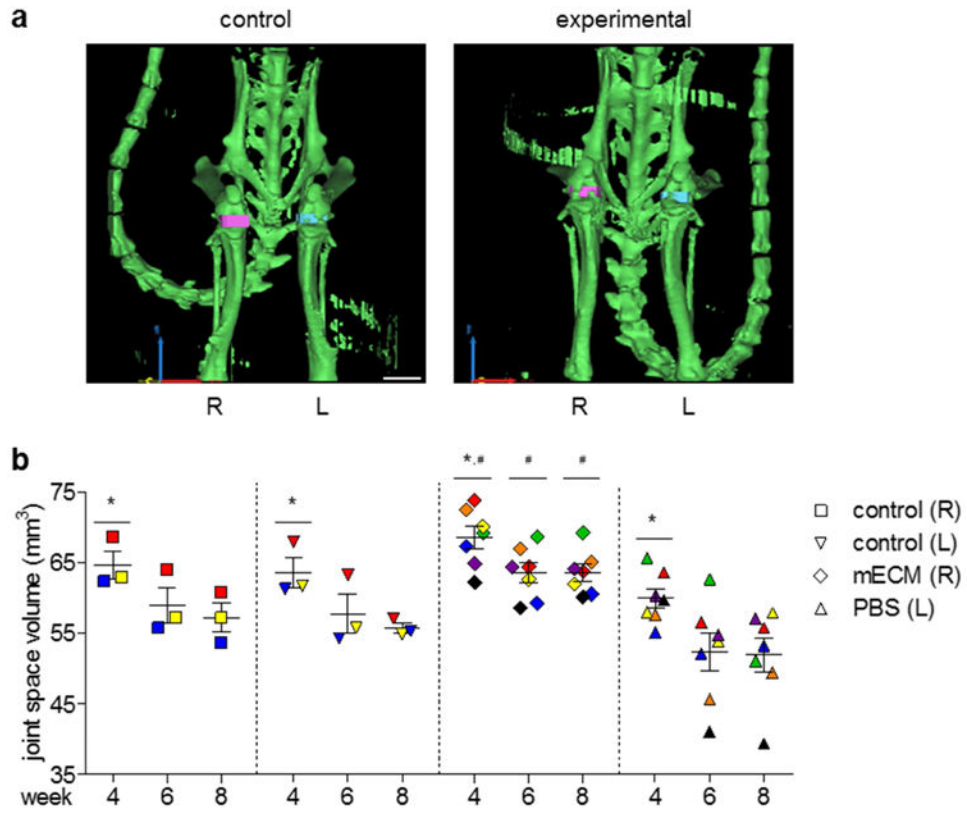


**Figure 8. Knees treated with hMSCs delivered in mECM hydrogel after meniscal injury *in vivo* show greater preservation of the joint space between the distal femur and proximal tibia at late time points**

(a) Coronal views of 3D segmentation models of CT images from representative control and experimental animals at week 8, calculated from thresholding masks for bone (green), right joint space (pink), and left joint space (blue). Scale bar = 5 mm. *x-y-z* axes = red-yellow-blue. (b) Joint space volumes calculated from 3D segmentation models at weeks 4, 6, and 8 post-injury. Matched values from the left and right knees of individual animals indicated by color, with different colors representing different animals.  $n = 3-7$ . \*  $p < 0.05$  vs. week 8. #  $p < 0.05$  vs. PBS.